Arbitrary d-dimensional Pauli X gates of a flying qudit

Xiaoqin Gao,[1,2,3,4,*] Mario Krenn,[1,2,†] Jaroslav Kysela,[1,2] and Anton Zeilinger[1,2,‡]

[1]*Vienna Center for Quantum Science & Technology (VCQ), Faculty of Physics, University of Vienna, Boltzmanngasse 5, 1090 Vienna, Austria*

[2]*Institute for Quantum Optics and Quantum Information (IQOQI), Austrian Academy of Sciences, Boltzmanngasse 3, 1090 Vienna, Austria*

[3]*National Mobile Communications Research Laboratory, Southeast University, Sipailou 2, 210096 Nanjing, China*

[4]*Quantum Information Research Center of Southeast University, Southeast University, Sipailou 2, 210096 Nanjing, China*

(Received 6 November 2018; published 13 February 2019)

High-dimensional degrees of freedom of photons can encode more quantum information than their two-dimensional counterparts. While the increased information capacity has advantages in quantum applications (such as quantum communication), controlling and manipulating these systems has been challenging. Here we show a method to perform deterministic arbitrary high-dimensional Pauli X gates for single photons carrying orbital angular momentum. The X gate consists of a cyclic permutation of qudit basis vectors and, together with the Z gate, forms the basis for performing arbitrary transformations. The proposed experimental setups only use two basic optical elements such as mode sorters and mode shifters and thus could be implemented in any system where these experimental tools are available. Furthermore the number of involved interferometers scales logarithmically with the dimension, which is important for practical implementation.

DOI: 10.1103/PhysRevA.99.023825

I. INTRODUCTION

High-dimensional quantum systems allow for encoding, transmitting and processing more than one bit per photon. The exploitation of large alphabets in quantum communication protocols can significantly improve their capacity [1–3] and security [4,5]. However, performing well-defined manipulations in multilevel systems is significantly more challenging than for qubits. Schemes for implementation of an arbitrary unitary transformation were developed for the path degree of freedom (DoF) already in 1994 [6–8]. However, path-encoding schemes are very susceptible to phase changes and it is thus very challenging to use them in real-world quantum communication. Laguerre-Gaussian modes of light, carrying orbital angular momentum (OAM) [9,10], represent an alternative to polarization that has become a popular choice in experiments in a high-dimensional quantum domain [11–13]. The OAM of photons has been used successfully in long-distance classical [14–17] and quantum [3,18,19] communication in the form of a "flying qudit" (Unitary transformations are well known for qudits encoded in the path DoF [6]; however, path-encoded qudits cannot be used for long-distance free space communication. Therefore, flying qudits usually refer to the spatial DoF). An important open question is how an arbitrary high-dimensional transformation can be performed with OAM.

An arbitrary unitary transformation in a finite-dimensional space can be expressed as a combination of Pauli X and Z gates and their integer powers [20], which shows that they are important basis gates. The Z gate for OAM qudits introduces a mode-dependent phase, which can be implemented simply by a Dove prism [21–24]. The X gate in high-dimensional Hilbert spaces takes the form of a cyclic permutation of the computational basis vectors. For a fixed basis in a d-dimensional space the cyclic transformation transforms each basis state into its nearest neighbor in a clockwise manner with the last state being transformed back to the first one [25]. As such, the cyclic transformation is the dth root of unity that performs a rotation in a d-dimensional space. While efficient methods for realizing a four-dimensional cyclic transformation in both classical and quantum realms have been experimentally demonstrated [25–27], for an arbitrary dimension such methods are still missing.

Here we present setups of X gates for arbitrary d-dimensional qudits represented by the OAM of single photons. When developing the general method we took inspiration from designs generated by the computer program MELVIN [28]. Schemes produced by the method can be implemented in the laboratory using accessible optical components. The setups employ only two basic elements: holograms and OAM beam splitters (OAM-BSs) introduced by Leach *et al.* [21]. Importantly, the number of OAM-BSs (which are interferometric devices) scales logarithmically with the dimension of the cycle, which is relevant for their experimental implementation.

II. ARBITRARY d-DIMENSIONAL X GATES

The main goal of this paper is to find deterministic experimental setups for realizing arbitrary d-dimensional X gates with the OAM of single photons. We would like to perform

*xiaoqin.gao@univie.ac.at

†mario.krenn@univie.ac.at; present address: Department of Chemistry, University of Toronto, Toronto, Ontario M5S 3H6, Canada.

‡anton.zeilinger@univie.ac.at

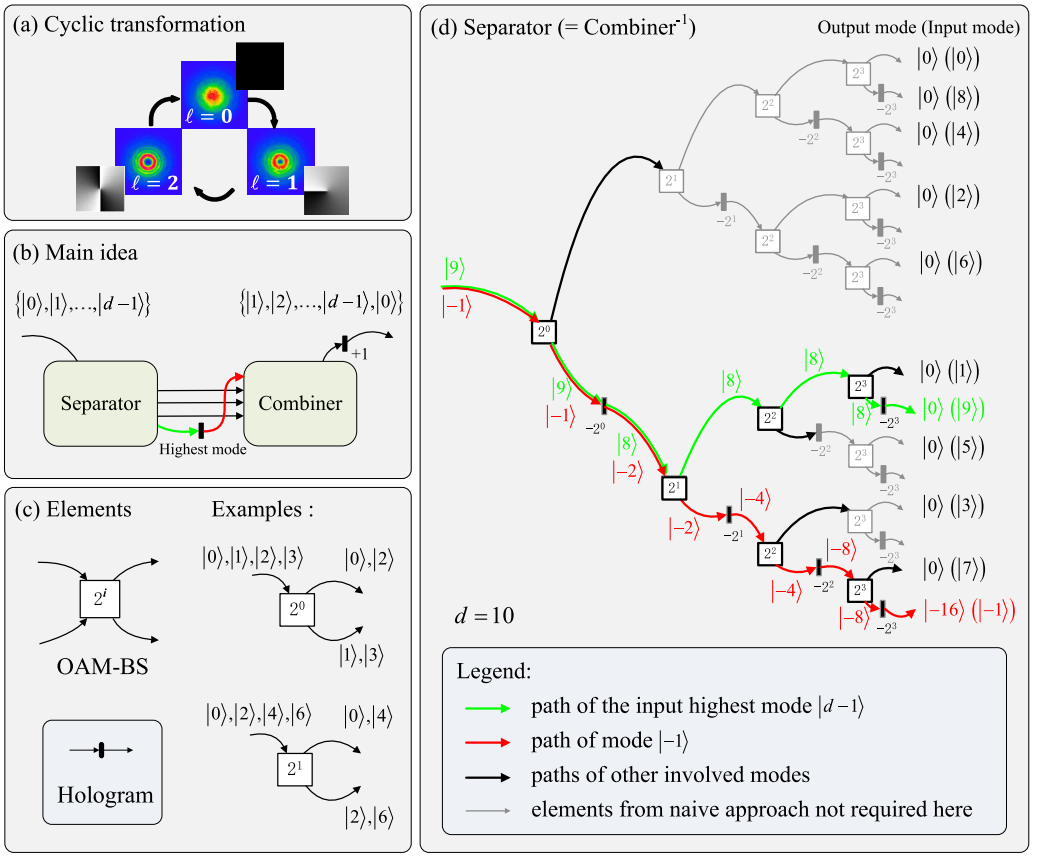

FIG. 1. Working principle of the general method. (a) The cyclic transformation in a three-dimensional space spanned by OAM modes $\ell = 0$, 1, and 2. If the incoming beam possesses OAM of $\ell = 0$ ($\ell = 1$), it becomes $\ell = 1$ ($\ell = 2$) after adding $+1$ to the mode. The highest OAM mode $\ell = 2$ is transformed into $\ell = 0$ by subtraction of 2 quanta of OAM. The experimentally obtained intensity profiles and computer-generated phase profiles of OAM modes in a beam cross section are inserted for convenience. (b) Main idea: The general setup is combined by a Separator, a Combiner, a $+1$ mode shifter, and an additional hologram that is inserted in the path of the highest mode. The Separator splits the modes $|d-1\rangle$ [green (light gray)] and $|-1\rangle$ [red (dark gray); it is an ancillary mode that is required in our scheme] into separate paths. Then the OAM of the highest mode is changed to $|-1\rangle$, and it enters the path of mode $|-1\rangle$. Subsequently, all modes are combined again by the Combiner into one path and acquire $+1$ quantum of OAM in the end. (c) Two basic elements: OAM-BSs and holograms. The label 2^i determines the sorting properties of the OAM-BSs. Holograms perform shifts of the OAM value by a fixed predefined amount. See Fig. 2 for details about the structure of the OAM-BS. (d) Separator: We choose the highest mode, $|9\rangle$ [green (light gray)], in the ten-dimensional cycle. Afterwards, it will enter into the lowest path of mode $|-1\rangle$. The Separator and the Combiner display a high degree of symmetry—they are mirror reflections of each other, with an inversion of hologram values. It is instructive to compare our scaling behavior with the naive approach, where $(d-1)$ OAM-BSs are used to reroute all d OAM modes into separate paths; d holograms are then used to shift the OAM values of all modes; and finally additional $(d-1)$ OAM-BSs are necessary to recombine all modes together. Our approach therefore offers a number of interferometers that is exponentially smaller than that of the naive approach.

an X gate that consists of a cyclic permutation of qudit basis vectors. One example is the cyclic transformation in three-dimensional space shown in Fig. 1(a), where the OAM mode $\ell = 0$ is transformed into $\ell = 1$, mode $\ell = 1$ into $\ell = 2$, and mode $\ell = 2$ back into $\ell = 0$. The main idea behind our approach is shown in Fig. 1(b): The setup consists of a Separator, a Combiner, a $+1$ mode shifter, and an additional mode shifter that works only for the highest mode. The Separator is used for splitting modes from one path to multiple paths, while the Combiner does the opposite, regrouping all modes into a single path. First, the input photon that is in the subspace spanned by the modes $|0\rangle, |1\rangle, |2\rangle, \ldots, |d-1\rangle$ goes through the Separator, which sends the highest mode to its own path. Subsequently, the highest mode acquires a mode shift and enters the path of mode $|-1\rangle$. Finally, the Combiner sends all modes into one single path and then a mode shifter adds $+1$ quantum of OAM. The Separator and the Combiner consist of multiple OAM-BSs and holograms, respectively, as shown in Fig. 1(c). The structure of the OAM-BS is depicted in Fig. 2. The Separator and the Combiner display a high degree of symmetry: The Combiner is a mirror reflection of the Separator, with an inversion of the hologram values.

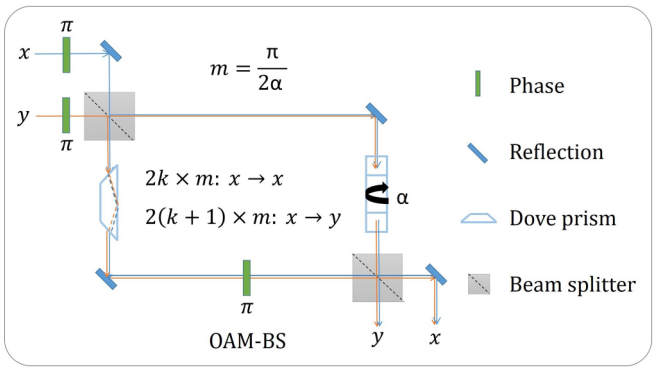

FIG. 2. OAM beam splitter, where x and y are input and output paths, respectively, and m specifies the angle of one Dove prism, $m = \pi/2\alpha$. If the input mode is $2k \times m$ ($k \in \mathbb{Z}$), the output path is the same as the input path. For $(2k+1) \times m$ it will go to the other path. For $m = 1$ the OAM-BS works as a parity sorter.

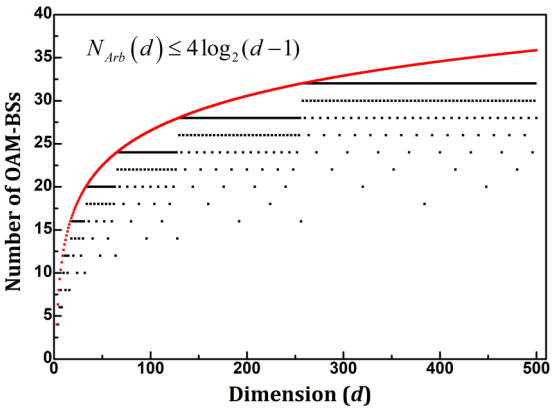

FIG. 3. The number of OAM-BSs scales logarithmically with the dimension d.

Except for the highest mode, all other modes only acquire $+1$ quantum of OAM in total. In our method, we only need to separate the path of mode $|-1\rangle$ and the path of the highest mode from all other modes. As an example, we show the ten-dimensional cycle in Fig. 1(d). The highest mode, $|9\rangle$, will enter the lowest path of mode $|-1\rangle$ [red (dark gray)] after going through a mode shift of -16 quanta of OAM. Due to the symmetry of the Separator and the Combiner, mode $|9\rangle$ will change to mode $|-1\rangle$ before the last mode shifter adds $+1$. Therefore, the highest mode ends up in mode $|0\rangle$, as required.

III. SCALING

The proposed experiments for X gates involve interferometers, which are demanding to stabilize experimentally. For that reason, a small number of interferometers is favorable. One naive approach to perform an X gate would be to transform the OAM information to path encoding by splitting every mode into its own path. This would require $2(d-1)$ interferometers, which is linear in the dimension. The strength of our method is that it requires only a logarithmical number of interferometers and thus is significantly easier to implement, especially for high dimensions.

Based on the main idea of Fig. 1, one can draw the setup with arbitrary dimension d. In general, the setup for the d-dimensional cycle is a combination of two different experimental structures, namely one for powers-of-two 2^M and one for odd number Q. The total dimension is given by

$$d = 2^M \times Q. \tag{1}$$

For example, the setup for the case $d = 88 = 8 \times 11$ is built up from two setups of dimension $d = 8$ and $d = 11$, see the Appendix.

Remarkably, the number N_{Arb} of OAM-BSs scales logarithmically with the dimension d, as follows

$$\begin{aligned} N_{\mathrm{Arb}}(d) &= N_{2^M}(d) + N_{\mathrm{Odd}}(d) \\ &= 2\{M(d) + 2\lfloor \log_2 Q(d) \rfloor\} \\ &\leqslant 4\log_2(d-1), \end{aligned} \tag{2}$$

These numbers are obtained with a slightly optimized setup, where for cycles with $Q > 1$ two unnecessary OAM-BSs and unnecessary holograms are removed. An algorithmic code to produce cyclic transformation setups for arbitrary d is shown in the Appendix. Additionally, the power-of-two, $M(d)$, and the odd part of an integer d, $Q(d)$, can be obtained using these elementary functions: $M(d) = \sum_{n=1}^{d} \{\lfloor \cos^2(\frac{d\pi}{2^n}) \rfloor\}$ and $Q(d) = \frac{d}{2^{M(d)}}$.

This is shown in Fig. 3, where the number N_{Arb} is plotted as a function of dimension d for $3 \leqslant d \leqslant 500$. For example, we can realize 500-dimensional cyclic transformation using a setup with only 28 OAM-BSs. Such a setup is already within reach of the present-day technology—recently an experiment has been reported [29] where 30 interferometers were kept stable over 72 h without any active stabilization.

Interestingly, for any given $M \geqslant 1$ and for all odd dimensions d in the range $2^M + 1, \ldots, 2^{M+1} - 1$, the number of OAM-BSs in the generated setups stays constant, as shown in Fig. 3, and only the connections between individual elements differ. For example, the number of OAM-BSs is 12 for all $d = 9$, 11, 13, and 15, as shown in the Appendix.

As an illustration, we depict the setup for the case $d = 10$ in Fig. 4. The Separator and the Combiner in Fig. 4(a) correspond to the main idea in Fig. 1. The propagation of three modes is shown explicitly in the figure in order to illustrate how the experimental implementation works. The crucial property of the setup is that only the highest-order mode propagates through the center; hence it undergoes an additional -2^3 OAM shift and then enters the lowest path of mode $|-1\rangle$ resulting in the transformation $|9\rangle \to |0\rangle$ after the last operation $+1$. If the path differences are matched such

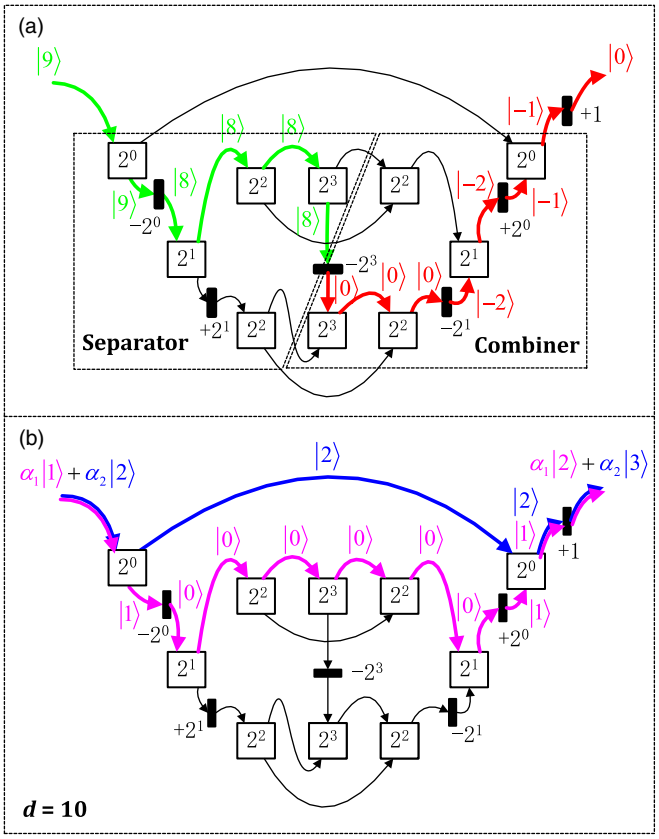

FIG. 4. (a) The experimental setup for the X gate in the ten-dimensional space. The Separator and the Combiner here correspond to the main idea in Fig. 1. Four different types of OAM-BSs and six holograms are used in the setup. Unlike other modes the highest-order mode, $|9\rangle$, propagates through the middle path and enters the path of mode $|-1\rangle$ after receiving a -2^3 mode shift. (b) The setup also works for a superposition, such as $|\psi_{\text{in}}\rangle = \alpha_1 |1\rangle + \alpha_2 |2\rangle$.

that they are smaller than the coherence length of the input, the setup also works for a superposition.

IV. CONCLUSION AND OUTLOOK

We developed a method for experimental setups realizing arbitrarily high-dimensional cyclic transformations with OAM of single photons. The total number of required interferometers scales logarithmically with the dimension. Given that a recent experiment has been demonstrated [29] with very high quality and stability of 30 interferometers, our method is experimentally feasible in high dimensions. A cyclic transformation in a given d-dimensional space is defined for a specific basis, $|0\rangle, |1\rangle, |2\rangle, \ldots, |d-1\rangle$, but also for other sets of states without adaptation of the experimental setup, which are shown in the Appendix. Furthermore, we can also get arbitrary d-dimensional cyclic transformations for OAM modes $|0+m\rangle, |1+m\rangle, |2+m\rangle, \ldots, |d-1+m\rangle$ if we put one hologram with value m before the setup and another hologram with the opposite value, $-m$, after the setup. The structure of the setups generated by our method is very symmetric. Consequently, if the photon has a sufficiently large coherence length, the original setup can be considerably simplified. This is shown in the Appendix. Implementations of X gates generated by the method presented here have a very convenient property that they can be converted into the X^{-1}-gate implementations only by a modification of two holograms and slight reconnection of two OAM-BSs, as shown in the Appendix. This is beneficial in future implementations, where quick automated changes between gates are necessary. There are still some very interesting emerging questions.

To experimentally create arbitrary unitary transformations one needs to combine all of the $X^l Z^m$ building blocks. This recombination can be performed in the probabilistic way, which leads to losses. An important immediate question is how our results can be generalized so that broader classes of transformations can be realized in a deterministic manner.

The high-dimensional generalized controlled-NOT (CNOT) gate is a controlled cyclic gate. Realizing arbitrary d-dimensional CNOT gates in the OAM would be very desirable, as it allows for more complex control and processing of multiphotonic states.

The method works in principle in any quantum system where experimental tools for mode sorting and mode shifting exist. In particular, the full transverse structure of photons consists of the orbital angular momentum mode (investigated here) and the radial mode (p mode) [30,31]. Lossless mode sorters for radial modes have recently been implemented [32,33]. Thus, in order to generalize our result to radial modes, one requires a method to increase the mode number of radial modes—which is an interesting path for future research.

Our scheme for implementing arbitrarily-dimensional X gates was discovered by interpreting and generalizing the special-case method found by the computer program MELVIN [28]. Various other computer programs have recently been developed to autonomously find, optimize, or simplify quantum experiments [34–36]. It is exciting to think about how a computer program itself would be able to generalize the special-case method in a manner similar to that of human intelligence.

ACKNOWLEDGMENTS

The authors thank Giuseppe Vitagliano, Nicolai Friis, Jessica Bavaresco, and Maximilian Lock for helpful discussions. X.G. thanks Bin Sheng and Zaichen Zhang for support. This work was supported by the Austrian Academy of Sciences (ÖAW) and the Austrian Science Fund (FWF) with SFB F40 (FOQUS) and W 1210-N25 (CoQuS). X.G. acknowledges support from the National Natural Science Foundation of China (Grants No. 61571105, No. 61501109, and No. 61601119), the Scientific Research Foundation of Graduate School of Southeast University (Grant No. YBJJ1710), and the China Scholarship Council (CSC).

APPENDIX

1. Pseudocodes

Algorithm 1. Pseudocode for arbitrary dimension

Assume: The input state is a linear combination of modes $|0\rangle, |1\rangle, |2\rangle, \ldots, |d-1\rangle$ and enters the first path r_0.
Assume: $LI_m(x, y)$ stands for an OAM-BS, where m determines into which paths (x or y) individual OAM modes are output, as shown in Fig. 1(c).
Assume: $Holog(p, v)$ stands for a hologram in path p that adds value v to the OAM mode. It is shown in Fig. 1(c).
Assume: N and b_t are calculated from $Q = \sum_{i=0}^{N-1}(b_i \times 2^i)$, $b_i = 0$ and 1. M is calculated by $d = 2^M \times Q$.
Assume: Auxiliary indices a_i are defined as
  $a_1 = 0$
  for t from 1 to $N-2$ **do**
    if $b_t = 0$ **then**
      $a_{t+1} = a_t$
    else
      $a_{t+1} = t$
    end if
  end for
  procedure CYCLE FOR ARBITRARY DIMENSION
    for t from 0 to $M-1$ **do**
      $LI_{2^t}(r_t, r_{t+1})$
      $Holog(r_{t+1}, -2^t)$
    end for
    if $N = 1$ **then**
      $Holog(r_M, -2^M)$
    else
      $LI_{2^M}(r_M, s_0)$
      $Holog(s_0, +2^M)$
      for t from 1 to $N-2$ **do**
        $LI_{2^{t+M}}(r_{a_t+M}, r_{t+M})$
        $Holog(r_{t+M}, -b_t \times 2^{t+M})$
      end for
      $LI_{2^{N-1+M}}(r_{a_{N-1}+M}, r_{N-1+M})$
      $Holog(r_{N-1+M}, -2^{N-1+M})$
      for t from $N-2$ down to 1 **do**
        $Holog(r_{t+M}, +b_t \times 2^{t+M})$
        $LI_{2^{t+M}}(r_{a_t+M}, r_{t+M})$
      end for
      for t from 1 to $N-2$ **do**
        $LI_{2^{t+M}}(s_0, s_t)$
      end for
      $LI_{2^{N-1+M}}(r_{N-1+M}, s_0)$
      for t from $N-2$ down to 1 **do**
        $LI_{2^{t+M}}(r_{N-1+M}, s_t)$
      end for
      $Holog(r_{N-1+M}, -2^M)$
      $LI_{2^M}(r_M, r_{N-1+M})$
    end if
    for t from $M-1$ down to 0 **do**
      $Holog(r_{t+1}, +2^t)$
      $LI_{2^t}(r_t, r_{t+1})$
    end for
    $Holog(r_0, +1)$
  end procedure

Algorithm 2. Special case—Pseudocode for odd dimension

Assume: The input state is a linear combination of modes $|0\rangle, |1\rangle, |2\rangle, \ldots, |d-1\rangle$ and enters the first path r_0.
Assume: $LI_m(x, y)$ stands for an OAM-BS, where m determines into which paths (x or y) individual OAM modes are output, as shown in Fig. 1(c).
Assume: Holog(p, v) stands for a hologram in path p that adds value v to the OAM mode. It is shown in Fig. 1(c).
Assume: N and b_t are calculated via $d = \sum_{i=0}^{N-1}(b_i \times 2^i)$, $b_i = 0$ and 1.
Assume: Auxiliary indices a_i are defined as
  $a_1 = 0$
  for t from 1 to $N-2$ **do**
    if $b_t = 0$ **then**
      $a_{t+1} = a_t$
    else
      $a_{t+1} = t$
    end if
  end for
  procedure CYCLE FOR ODD DIMENSION
    $LI_{2^0}(r_0, s_0)$
    $Holog(s_0, +1)$
    for t from 1 to $N-2$ **do**
      $LI_{2^t}(r_{a_t}, r_t)$
      $Holog(r_t, -b_t \times 2^t)$
    end for
    $LI_{2^{N-1}}(r_{a_{N-1}}, r_{N-1})$
    $Holog(r_{N-1}, -2^{N-1})$
    for t from $N-2$ down to 1 **do**
      $Holog(r_t, +b_t \times 2^t)$
      $LI_{2^t}(r_{a_t}, r_t)$
    end for
    for t from 1 to $N-2$ **do**
      $LI_{2^t}(s_0, s_t)$
    end for
    $LI_{2^{N-1}}(r_{N-1}, s_0)$
    for t from $N-2$ down to 1 **do**
      $LI_{2^t}(r_{N-1}, s_t)$
    end for
    $Holog(r_{N-1}, -1)$
    $LI_{2^0}(r_0, r_{N-1})$
    $Holog(r_0, +1)$
  end procedure

2. Structure of setup

The general setup for the d-dimensional cycle is combined by two different structures of powers-of-two 2^M and odd number Q. The total dimension is expressed by Eq. (1). For example, the setup for $d = 88 = 8 \times 11$ is combined by two setups of dimension $d = 8$ and $d = 11$. As shown in Fig. 5.

Interestingly, the number of OAM-BSs in the generated setups for all odd dimensions between $2^M + 1$ and $2^{M+1} - 1$ keeps constant, as shown in Fig. 3. For example, the number of OAM-BSs is 12 for all $d = 9$, 11, 13, and 15, as shown in Fig. 6.

3. Different basis states

The experimental setup shown in Fig. 5(d) implements the 11-dimensional cyclic transformation not only for states

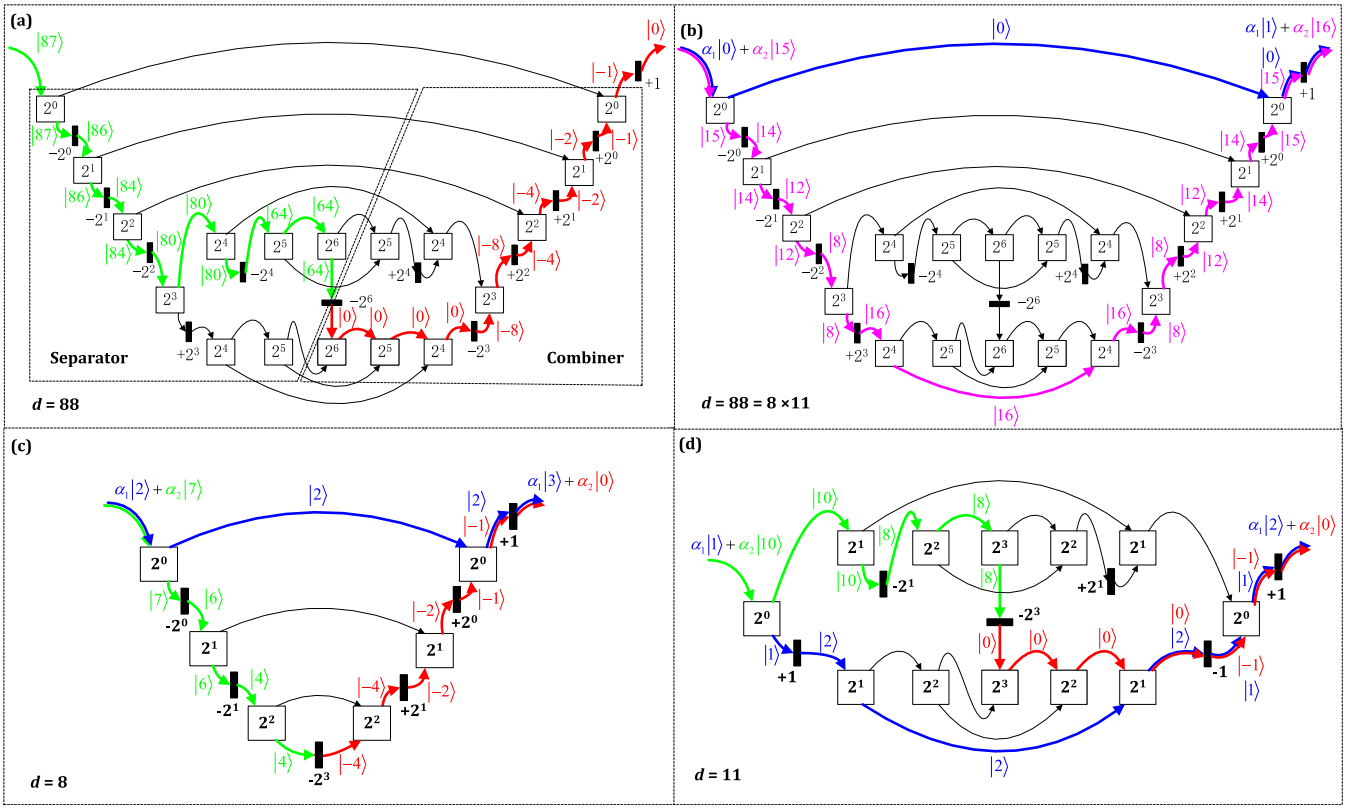

FIG. 5. (a) The experimental setup for the X gate in the 88-dimensional space. That is $d = 88$, for which $M = 3$ and $Q = 11$ according to $d = 2^M \times Q$. The setup is a combination of setups for $d = 8$ and $d = 11$. Unlike other modes the highest-order mode, $|87\rangle$, propagates through the middle path and enters the path of mode $|-1\rangle$. There are only 18 OAM-BSs in the setup for $d = 88$. (b) The setup works for a superposition, such as $|\psi_{\text{in}}\rangle = \alpha_1 |0\rangle + \alpha_2 |15\rangle$. (c) The experimental setup for realization of the X gate in an 8-dimensional space. The setup works for an arbitrary complex linear combination of modes $|0\rangle$ through $|7\rangle$. For example, the input state $|\psi_{\text{in}}\rangle = \alpha_1 |2\rangle + \alpha_2 |7\rangle$ is transformed into the output state $|\psi_{\text{out}}\rangle = \alpha_1 |3\rangle + \alpha_2 |0\rangle$. (d) The experimental setup for the X gate in dimension $d = 11$. The device works for coherent superposition, as is shown for the example $|\psi_{\text{in}}\rangle = \alpha_1 |1\rangle + \alpha_2 |10\rangle$.

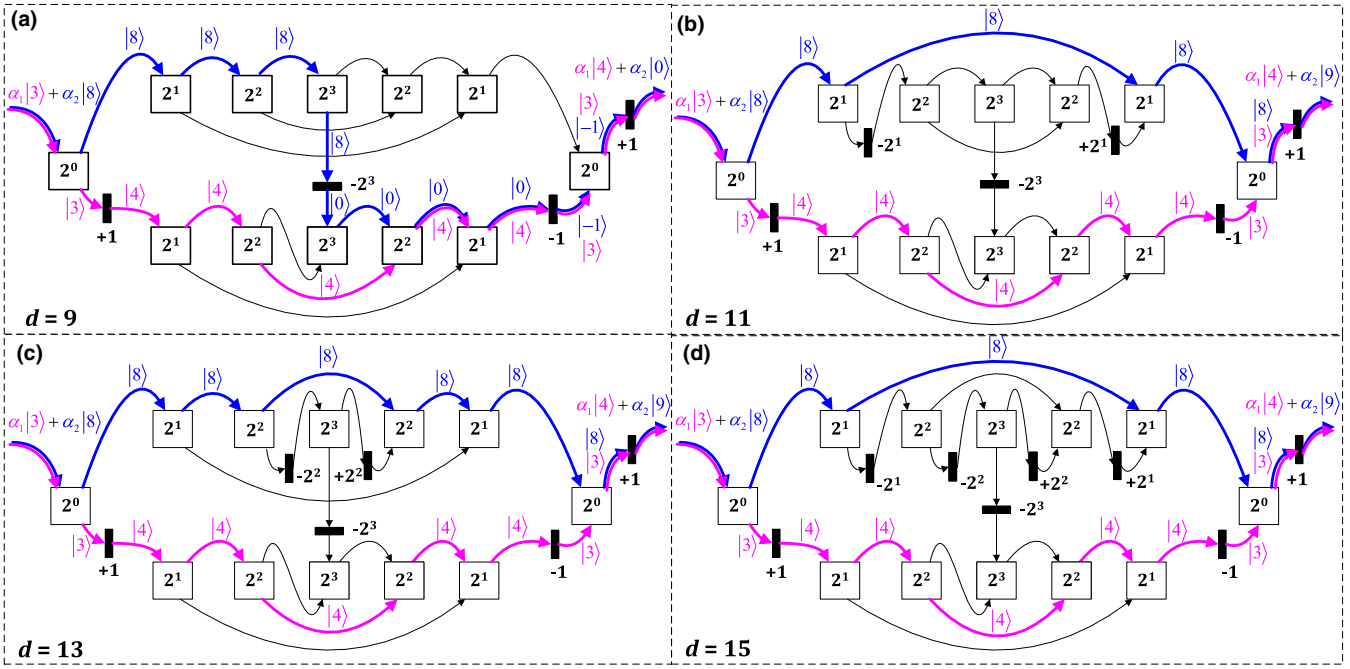

FIG. 6. (a)–(d) The experimental setups for the X gate in dimensions $d = 9$, 11, 13, and 15, respectively. The number of OAM-BS is 12 in all cases. While individual elements are connected differently in each setup, the overall structure does not change. The superposition $\alpha_1 |3\rangle + \alpha_2 |8\rangle$ goes through different paths in different setups.

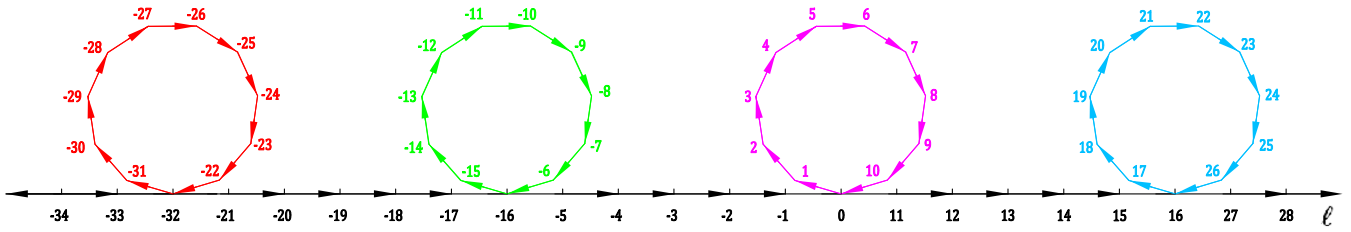

FIG. 7. Possible 11-dimensional cyclic transformations implemented by the setup in Fig. 5(d). Each closed hendecagon shows the set of 11 OAM modes that can be cycled through with our experimental setup.

Algorithm 3. Special case—Pseudocode for power-of-two dimension

Assume: The input state is a linear combination of modes $|0\rangle, |1\rangle, |2\rangle, \ldots, |d-1\rangle$ and enters the first path r_0.
Assume: $LI_m(x, y)$ stands for an OAM-BS, where m determines into which paths (x or y) individual OAM modes are output, as shown in Fig. 1(c).
Assume: Holog(p, v) stands for a hologram in path p that adds value v to the OAM mode. It is shown in Fig. 1(c).
Assume: $M = \log_2 d$.
  procedure CYCLE FOR 2^M DIMENSION
    for t from 0 to $M-1$ **do**
      $LI_{2^t}(r_t, r_{t+1})$
      $Holog(r_{t+1}, -2^t)$
    end for
    $Holog(r_M, -2^M)$
    for t from $M-1$ down to 0 **do**
      $Holog(r_{t+1}, +2^t)$
      $LI_{2^t}(r_t, r_{t+1})$
    end for
    $Holog(r_0, +1)$
  end procedure

$|0\rangle, \ldots, |10\rangle$ but also for infinitely many additional sets of states, three of which are shown in Fig. 7. This feature also exists in other dimensions.

4. Simplification

The structure of setups generated by Algorithm 1 and demonstrated in Fig. 5 is very symmetric—in the first part individual modes entering the setup are rerouted into different paths, the second part treats the highest mode separately from the other modes, and finally the third part again recombines all modes into a single output path. Similarity of the third, recombination, part and the first, rerouting, part allows us to remove the third part altogether. Provided that the photon has a sufficiently large coherence length the original setup can be simplified considerably.

As an example, we suppose that the photon has sufficiently long coherence length and simplify the 11-dimensional cycle in Fig. 5(d). Four OAM-BSs can thus be removed and paths leading to them are reconnected as demonstrated by red (dark gray) and green (light gray) lines in Fig. 8. The number of OAM-BSs for dimension $d = 11$ is thus reduced from 12 to 8. For dimension 500, such a simplification leads to a reduction from 28 to 16. In general, the total number of OAM-BSs used in the simplified setup is equal to

$$N_S = M + 2\lfloor \log_2 Q \rfloor + 2, \tag{A1}$$

which is approximately a half of the OAM beam splitters used in the original setup [cf. Eq. (2)]. Even though the scaling is still logarithmic, especially for high-dimensional cyclic transformations the reduction in complexity of actual experimental setups may be of great usefulness.

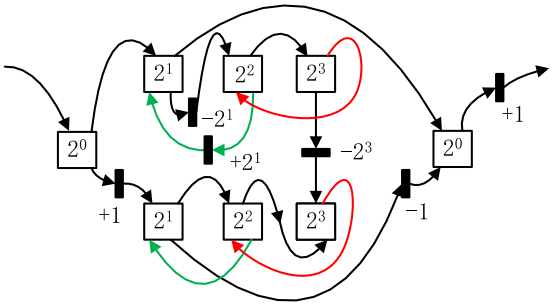

FIG. 8. The simplified experimental setup implementing the 11-dimensional cycle. In Fig. 5(d), the right part is not necessary as the left part can be used both to reroute and to recombine individual OAM modes.

5. X^{-1} gate

In Fig. 9 one can see the setup for the X^{-1} gate in the 88-dimensional Hilbert space, where differences from the implementation of the corresponding X gate in Fig. 5 are highlighted.

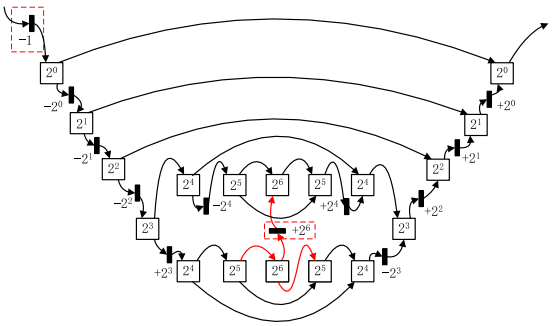

FIG. 9. The X^{-1} gate implementation in the 88-dimensional state space. The differences from the implementation of the X-gate in Fig. 5 are highlighted. Specifically, the final hologram is moved to the beginning, the central hologram is inverted and two central OAM-BSs are connected differently to their neighbors and to each other.

[1] S. Gröblacher, T. Jennewein, A. Vaziri, G. Weihs, and A. Zeilinger, Experimental quantum cryptography with qutrits, New J. Phys. **8**, 75 (2006).

[2] M. Mirhosseini, O. S. Magaña-Loaiza, M. N. O'Sullivan, B. Rodenburg, M. Malik, M. P. Lavery, M. J. Padgett, D. J. Gauthier, and R. W. Boyd, High-dimensional quantum cryptography with twisted light, New J. Phys. **17**, 033033 (2015).

[3] A. Sit, F. Bouchard, R. Fickler, J. Gagnon-Bischoff, H. Larocque, K. Heshami, D. Elser, C. Peuntinger, K. Günthner, B. Heim *et al.*, High-dimensional intracity quantum cryptography with structured photons, Optica **4**, 1006 (2017).

[4] M. Huber and M. Pawłowski, Weak randomness in device-independent quantum key distribution and the advantage of using high-dimensional entanglement, Phys. Rev. A **88**, 032309 (2013).

[5] F. Bouchard, R. Fickler, R. W. Boyd, and E. Karimi, High-dimensional quantum cloning and applications to quantum hacking, Sci. Adv. **3**, e1601915 (2017).

[6] M. Reck, A. Zeilinger, H. J. Bernstein, and P. Bertani, Experimental Realization of Any Discrete Unitary Operator, Phys. Rev. Lett. **73**, 58 (1994).

[7] J. Carolan, C. Harrold, C. Sparrow, E. Martín-López, N. J. Russell, J. W. Silverstone, P. J. Shadbolt, N. Matsuda, M. Oguma, M. Itoh *et al.*, Universal linear optics, Science **349**, 711 (2015).

[8] C. Schaeff, R. Polster, M. Huber, S. Ramelow, and A. Zeilinger, Experimental access to higher-dimensional entangled quantum systems using integrated optics, Optica **2**, 523 (2015).

[9] L. Allen, M. W. Beijersbergen, R. Spreeuw, and J. Woerdman, Orbital angular momentum of light and the transformation of Laguerre-Gaussian laser modes, Phys. Rev. A **45**, 8185 (1992).

[10] M. J. Padgett, Orbital angular momentum 25 years on, Opt. Express **25**, 11265 (2017).

[11] A. Mair, A. Vaziri, G. Weihs, and A. Zeilinger, Entanglement of the orbital angular momentum states of photons, Nature (London) **412**, 313 (2001).

[12] H. Rubinsztein-Dunlop, A. Forbes, M. V. Berry, M. R. Dennis, D. L. Andrews, M. Mansuripur, C. Denz, C. Alpmann, P. Banzer, T. Bauer *et al.*, Roadmap on structured light, J. Opt. **19**, 013001 (2016).

[13] M. Erhard, R. Fickler, M. Krenn, and A. Zeilinger, Twisted photons: New quantum perspectives in high dimensions, Light: Science and Applications **7**, 17146 (2018).

[14] M. Krenn, R. Fickler, M. Fink, J. Handsteiner, M. Malik, T. Scheidl, R. Ursin, and A. Zeilinger, Communication with spatially modulated light through turbulent air across Vienna, New J. Phys. **16**, 113028 (2014).

[15] M. Krenn, J. Handsteiner, M. Fink, R. Fickler, R. Ursin, M. Malik, and A. Zeilinger, Twisted light transmission over 143 km, Proc. Natl. Acad. Sci. USA **113**, 13648 (2016).

[16] Y. Ren, Z. Wang, P. Liao, L. Li, G. Xie, H. Huang, Z. Zhao, Y. Yan, N. Ahmed, A. Willner *et al.*, Experimental characterization of a 400 Gbit/s orbital angular momentum multiplexed free-space optical link over 120 m, Opt. Lett. **41**, 622 (2016).

[17] M. P. Lavery, C. Peuntinger, K. Günthner, P. Banzer, D. Elser, R. W. Boyd, M. J. Padgett, C. Marquardt, and G. Leuchs, Free-space propagation of high-dimensional structured optical fields in an urban environment, Sci. Adv. **3**, e1700552 (2017).

[18] M. Krenn, J. Handsteiner, M. Fink, R. Fickler, and A. Zeilinger, Twisted photon entanglement through turbulent air across Vienna, Proc. Natl. Acad. Sci. USA **112**, 14197 (2015).

[19] F. Bouchard, A. Sit, F. Hufnagel, A. Abbas, Y. Zhang, K. Heshami, R. Fickler, C. Marquardt, G. Leuchs, R. Boyd, and E. Karimi, Quantum cryptography with twisted photons through an outdoor underwater channel, Opt. Express **26**, 22563 (2018).

[20] A. Asadian, P. Erker, M. Huber, and C. Klöckl, Heisenberg-Weyl Observables: Bloch vectors in phase space, Phys. Rev. A **94**, 010301(R) (2016).

[21] J. Leach, M. J. Padgett, S. M. Barnett, S. Franke-Arnold, and J. Courtial, Measuring the Orbital Angular Momentum of a Single Photon, Phys. Rev. Lett. **88**, 257901 (2002).

[22] N. González, G. Molina-Terriza, and J. P. Torres, How a Dove prism transforms the orbital angular momentum of a light beam, Opt. Express **14**, 9093 (2006).

[23] M. Agnew, J. Z. Salvail, J. Leach, and R. W. Boyd, Generation of Orbital Angular Momentum Bell States and Their Verification via Accessible Nonlinear Witnesses, Phys. Rev. Lett. **111**, 030402 (2013).

[24] Y. Zhang, F. S. Roux, T. Konrad, M. Agnew, J. Leach, and A. Forbes, Engineering two-photon high-dimensional states through quantum interference, Sci. Adv. **2**, e1501165 (2016).

[25] F. Schlederer, M. Krenn, R. Fickler, M. Malik, and A. Zeilinger, Cyclic transformation of orbital angular momentum modes, New J. Phys. **18**, 043019 (2016).

[26] A. Babazadeh, M. Erhard, F. Wang, M. Malik, R. Nouroozi, M. Krenn, and A. Zeilinger, High-Dimensional Single-Photon Quantum Gates: Concepts and Experiments, Phys. Rev. Lett. **119**, 180510 (2017).

[27] F. Wang, M. Erhard, A. Babazadeh, M. Malik, M. Krenn, and A. Zeilinger, Generation of the complete four-dimensional Bell basis, Optica **4**, 1462 (2017).

[28] M. Krenn, M. Malik, R. Fickler, R. Lapkiewicz, and A. Zeilinger, Automated Search for New Quantum Experiments, Phys. Rev. Lett. **116**, 090405 (2016).

[29] X. L. Wang, Y. H. Luo, H. L. Huang, M. C. Chen, Z. E. Su, C. Liu, C. Chen, W. Li, Y. Q. Fang, X. Jiang *et al.*, 18-Qubit Entanglement with Six Photons' Three Degrees of Freedom, Phys. Rev. Lett. **120**, 260502 (2018).

[30] E. Karimi, R. Boyd, P. De La Hoz, H. De Guise, J. Řeháček, Z. Hradil, A. Aiello, G. Leuchs, and L. L. Sánchez-Soto, Radial quantum number of Laguerre-Gauss modes, Phys. Rev. A **89**, 063813 (2014).

[31] W. N. Plick and M. Krenn, Physical meaning of the radial index of Laguerre-Gauss beams, Phys. Rev. A **92**, 063841 (2015).

[32] Y. Zhou, M. Mirhosseini, D. Fu, J. Zhao, S. M. H. Rafsanjani, A. E. Willner, and R. W. Boyd, Sorting Photons by Radial Quantum Number, Phys. Rev. Lett. **119**, 263602 (2017).

[33] X. Gu, M. Krenn, M. Erhard, and A. Zeilinger, Gouy Phase Radial Mode Sorter for Light: Concepts and Experiments, Phys. Rev. Lett. **120**, 103601 (2018).

[34] P. Knott, A search algorithm for quantum state engineering and metrology, New J. Phys. **18**, 073033 (2016).

[35] A. A. Melnikov, H. P. Nautrup, M. Krenn, V. Dunjko, M. Tiersch, A. Zeilinger, and H. J. Briegel, Active learning machine learns to create new quantum experiments, Proc. Natl. Acad. Sci. USA **115**, 1221 (2018).

[36] J. M. Arrazola, T. R. Bromley, J. Izaac, C. R. Myers, K. Brádler, and N. Killoran, Machine learning method for state preparation and gate synthesis on photonic quantum computers, Quantum Sci. Technol. **4**, 024004 (2019).